

**A NUMERICAL STUDIES ON THE EFFECT OF FLUID FLOW PATTERN  
IN THE CENTRIFUGAL PUMP AND ITS PERFORMANCE**

**YU CAI HONG**

**A project report submitted in partial fulfilment of the  
requirements for the award of Master of Engineering  
(Mechanical)**

**Lee Kong Chian Faculty of Engineering and Science  
Universiti Tunku Abdul Rahman**

**August 2016**

## DECLARATION

I hereby declare that this project report is based on my original work except for citations and quotations which have been duly acknowledged. I also declare that it has not been previously and concurrently submitted for any other degree or award at UTAR or other institutions.

Signature : \_\_\_\_\_

Name : \_\_\_\_\_

ID No. : \_\_\_\_\_

Date : \_\_\_\_\_

**APPROVAL FOR SUBMISSION**

I certify that this project report entitled “**A NUMERICAL STUDIES ON THE EFFECT OF FLUID FLOW PATTERN IN THE CENTRIFUGAL PUMP AND ITS PERFORMANCE**” was prepared by **YU CAI HONG** has met the required standard for submission in partial fulfilment of the requirements for the award of Master of Engineering (Mechanical) at Universiti Tunku Abdul Rahman.

Approved by,

Signature : \_\_\_\_\_

Supervisor : \_\_\_\_\_

Date : \_\_\_\_\_

The copyright of this report belongs to the author under the terms of the copyright Act 1987 as qualified by Intellectual Property Policy of Universiti Tunku Abdul Rahman. Due acknowledgement shall always be made of the use of any material contained in, or derived from, this report.

© 2016, Yu Cai Hong. All right reserved.

## ACKNOWLEDGEMENTS

This project would not be completed without the guidance and help of several individuals who have contributed and extended their assistance in preparation and completion of this study.

I would like to express my very great gratitude to my supervisor, Mr. King Yeong Jin for his patient guidance, enthusiastic and useful critics during the planning and execution of this research.

I would also like to thank everyone who have aided me in problems that I have encountered when carrying out the research

**A NUMERICAL STUDIES ON THE EFFECT OF FLUID FLOW PATTERN  
IN THE CENTRIFUGAL PUMP AND ITS PERFORMANCE**

**ABSTRACT**

This study aims to develop a comprehensive CFD model to simulate and predict the fluid flow pattern in a centrifugal pump impeller to optimize the performance of the pump. Unsteady flow in pump occurs frequently due to site conditions and pump design that causes pump to run at an off design condition. Hence, the flow pattern will causes fluctuation in pressure distribution on the pump and causes vibrations, cavitation or secondary flow. Thus, the effect of the pump impeller design specification on the fluid flow pattern will be computed using CFD modelling. The impeller dimension and blade angle will be varied to study on different scenario. The study is expected to be able to find out a better impeller design that can reduce the occurrence of unsteady flow and able to prolong the operating life of the pumpset. The study found that the impeller performance can be improved through the modification on the inlet dimension. Other than that, the blade angle can also be altered to achieve a better fluid flow pattern in an impeller.

**TABLE OF CONTENTS**

<b>DECLARATION</b>	<b>1</b>
<b>APPROVAL FOR SUBMISSION</b>	<b>2</b>
<b>ACKNOWLEDGEMENTS</b>	<b>4</b>
<b>ABSTRACT</b>	<b>5</b>
<b>TABLE OF CONTENTS</b>	<b>6</b>
<b>LIST OF TABLES</b>	<b>8</b>
<b>LIST OF FIGURES</b>	<b>9</b>

**CHAPTER**

<b>1</b>	<b>INTRODUCTION</b>	<b>11</b>
	1.1 Background	11
	1.2 Problem Statement	14
	1.3 Aim and Objectives	15
<b>2</b>	<b>LITERATURE REVIEW</b>	<b>16</b>
	2.1 Pump Flow	16
<b>3</b>	<b>METHODOLOGY</b>	<b>19</b>
	3.1 Modelling	19
	3.2 Meshing	22
	3.3 Setup	23
	3.4 Solver & Results	23
	3.5 Repeat	24
<b>4</b>	<b>RESULTS AND DISCUSSION</b>	<b>25</b>
	4.1 Base Model	25
	4.2 Transient Model	31

		7
4.3	Reduction of Inlet	34
4.4	Enlargement of outlet	39
4.5	Reduced Blade Angle	44
<b>5</b>	<b>CONCLUSION AND RECOMMENDATIONS</b>	<b>47</b>
5.1	Conclusion	47
	5.1.1 Recommendation	47
<b>5</b>	<b>REFERENCES</b>	<b>48</b>

**LIST OF TABLES**

<b>Tables</b>	<b>Page</b>
TABLE 1: BLADE SPECIFICATION	19
TABLE 2: MESH INFORMATION	22
TABLE 3: MESH STATISTICS	22
TABLE 4: PUMP CURVE DATA FOR BASE PUMP	25
TABLE 5: PUMP CURVE DATA FOR REDUCED 10MM PUMP	36
TABLE 6: PUMP CURVE DATA FOR REDUCED 20MM PUMP	37
TABLE 7: PUMP CURVE DATA FOR ENLARGED 10MM PUMP	41
TABLE 8: PUMP CURVE DATA FOR ENLARGED 20MM PUMP	42

## LIST OF FIGURES

<b>FIGURE</b>	<b>PAGE</b>
FIGURE 1: CENTRIFUGAL PUMP (HENSHAW, 2015)	11
FIGURE 2: PUMP OPERATION CURVE	12
FIGURE 3: VISTA CPD BLADE DESIGN	20
FIGURE 4: BLADEGEN	21
FIGURE 5: PUMP IMPELLER MODEL	21
FIGURE 6: MESHING OF IMPELLER	22
FIGURE 7: BASE PUMP CURVE	26
FIGURE 8: GRUNDFOS PUMP CURVE	26
FIGURE 9: BASE PUMP EFFICIENCY CURVE	27
FIGURE 10: TOTAL PRESSURE CONTOUR OF THE FLUID IN THE IMPELLER	28
FIGURE 11: VELOCITY DISTRIBUTION AT 20% SPAN	29
FIGURE 12: VELOCITY DISTRIBUTION AT 50% SPAN	29
FIGURE 13: VELOCITY DISTRIBUTION AT 80% SPAN	30
FIGURE 14: TOTAL PRESSURE CONTOUR OF THE FLUID IN THE IMPELLER	31
FIGURE 15: VELOCITY DISTRIBUTION AT 20% SPAN	32
FIGURE 16: VELOCITY DISTRIBUTION AT 50% SPAN	32
FIGURE 17: VELOCITY DISTRIBUTION AT 80% SPAN	33
FIGURE 18: TOTAL PRESSURE DISTRIBUTION IN REDUCED INLET 10MM(A) AND REDUCED INLET 20MM(B)	34
FIGURE 19: VELOCITY DISTRIBUTION AT 20% SPAN FOR REDUCED INLET 10MM(A) & REDUCED INLET 20MM(B)	34
FIGURE 20: VELOCITY DISTRIBUTION AT 50% SPAN FOR REDUCED INLET 10MM(A) & REDUCED INLET 20MM(B)	35
FIGURE 21: VELOCITY DISTRIBUTION AT 80% SPAN FOR REDUCED INLET 10MM(A) & REDUCED INLET 20MM(B)	35
FIGURE 22: REDUCED 10MM PUMP CURVE	36
FIGURE 23: REDUCED 10MM PUMP EFFICIENCY	37
FIGURE 24: REDUCED 20MM PUMP CURVE	38
FIGURE 25: REDUCED 20MM PUMP EFFICIENCY	38
FIGURE 26: TOTAL PRESSURE DISTRIBUTION FOR ENLARGED OUTLET 10MM(A) & ENLARGED OUTLET 20MM	39

FIGURE 27: VELOCITY DISTRIBUTION AT 20% SPAN FOR ENLARGED OUTLET 10MM(A) & ENLARGED OUTLET 20MM	39
FIGURE 28: VELOCITY DISTRIBUTION AT 50% SPAN FOR ENLARGED OUTLET 10MM(A) & ENLARGED OUTLET 20MM(B)	40
FIGURE 29: VELOCITY DISTRIBUTION AT 80% SPAN FOR ENLARGED OUTLET 10MM(A) & ENLARGED OUTLET 20MM(B)	40
FIGURE 30: ENLARGED 10MM PUMP CURVE	41
FIGURE 31: ENLARGED 10MM PUMP EFFICIENCY	42
FIGURE 32: ENLARGED 20MM PUMP CURVE	43
FIGURE 33: ENLARGED 20MM PUMP EFFICIENCY	43
FIGURE 34: TOTAL PRESSURE CONTOUR OF THE FLUID IN THE IMPELLER	44
FIGURE 35: VELOCITY DISTRIBUTION AT 20% SPAN	45
FIGURE 36: VELOCITY DISTRIBUTION AT 50% SPAN	45
FIGURE 37: VELOCITY DISTRIBUTION AT 80% SPAN	46



rotational motion of the impeller. This type of pump is commonly used in boosting the pressure of a fluid flow to transfer to a higher ground.

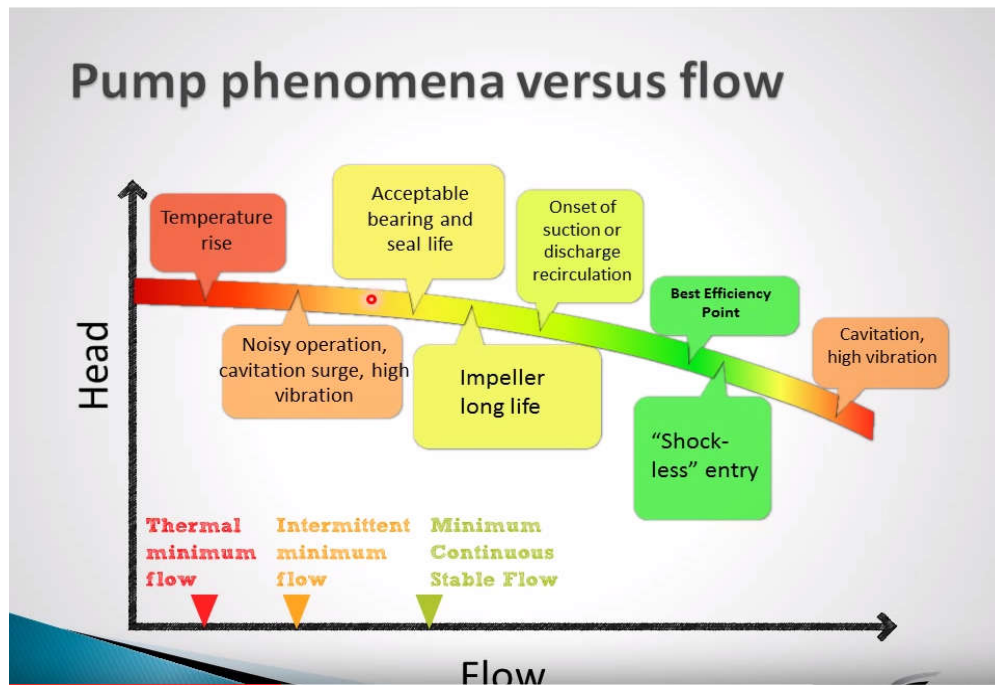


Figure 2: Pump Operation Curve

A pump will always operate within the range of a fixed pump curve as shown on figure 2 where it only perform best at the best efficiency point (BEP). When the pump operates outside of the optimum range, recirculation and cavitation will occurs. This is mainly due to the turbulent flow pattern in the pump itself.

There is a lack of research on the field of off design condition of a centrifugal pump. The study of fluid flow in pump is generally divided into different categories, namely, hydraulics, cavitation, vibration and machine arrangement. Among the four categories, the least studied field is the cavitation of the pump. The major contributor to this problem is the unsteady fluid induced pressure fluctuation within the pump. The difference generated by the pressure causes air bubble to form and implode on the

surface of the pump wall and causes cavitation. In this project, we will simulate by inducing steady flow into the pump and study the impact on the pump by varying the velocity and design of the impeller.

## 1.2 Problem Statement

The major problem involved in this study is the relatively small BEP region for the pump operation. When the pump is operating at the off design condition the motor and the impeller will be strained to fulfill the demand. When the process prolong, it will causes wastage of energy. It usually occurs when the sanitary fittings equipped by buildings are drawing more water than the pump is designed for. The higher water demand causes the design point further down the curve thus reducing the head produced, which will then leads to low output pressure on the sanitary fittings.

A pump has mainly 3 major components. Namely, a motor, impeller and volute. The motor drives the shaft (part of an impeller) to accelerates the fluid and discharge into a volute. The motor however, is selected based on the design capacity and the specification of both the impeller and volute. Other than that, volute is a casing which channels the outflow fluid direction and regulates the gradual change in pressure that are dependent on the discharge velocity and pressure generated from the impeller. Thus, the specification of the impeller plays a major role in the performance of a pump.

### **1.3 Aim and Objectives**

The aim of this project is to optimize the performance of a pump using computational fluid dynamics (CFD).

1. To simulate and predict the effect of fluid flow on the pump and its performance.
2. To develop an effective CFD model which is capable of accurately predicting and simulating the actual hydraulic problems in off design point centrifugal pump flow.
3. To be able to develop practical solutions to the fluid flow problems based on the CFD model.

## CHAPTER 2

### LITERATURE REVIEW

#### 2.1 Pump Flow

Gonzalez and Santolaria (2006) has studied on the unsteady flow structure and global variables in a centrifugal pump. In this study the fluid flow pattern was computed using the viscous incompressible Navier-Stokes equations that are solved within a 3D unsteady flow model. The equation used is proven to be very useful and is also employed by Barrio, Parrondo and Blanco (2010). Both of these researcher studies on the pressure fluctuation at the tongue region only. More detailed studies can be done on the impeller itself because it is the major component that translate the motion from the motor to the fluid. Hence, it will be included in this study.

According to studies done by Dong, Chu and Katz (1997), changing the impeller geometry will have a significant impact on the unsteady flow and performance efficiency of the pump. The impeller blade dimension was regulated to various thickness and there is an impact on the pressure distribution of the fluid flow in the pump. Other than that, Chakraborty and Pandey (2011) have also discovered that the pressure distribution is affected by the blade number of the centrifugal pump as well. It was found that the optimum number of blade for optimum efficiency is 10

number of blades running at 4000rpm. The study also discovered that the static pressure distribution at the screw section worsen with the increase in blade number, where as it is the otherwise for diffuser section.

One of the method that Gonzalez and Santolaria (2006) used to analyze the data obtained is the helicity of the fluid flow. According to Moffatt (2014), Helicity of a fluid is an invariant of the Euler equations of ideal fluid flow. It is depicted as the description of the knotness of the fluid flow in an unsteady flow. This is very important because the fluid flow properties involved in unsteady flow is turbulent flow. Despite that laminar flow has helicity, the effect of helicity on turbulent flow is more significant.

By referring to a computational studies done by Croba and Kueny in 1996, the interaction of the volute and impeller can be directly acquired through a multidomain overlapping grid technique to match the relative and absolute flow field. Researchers like Barrio, Parrondo and Blanco (2010) has used the SIMPLEC algorithm to couple the pressure and velocity field to compute the data.

To date, researchers has focused on the study of the near tongue region and the fluid chamber region in the pump rather than the impeller itself. Hence, the unsteady fluid flow effect on the centrifugal pump will be studied using CFD modelling, FLUENT with the consideration of number of blades, fluid helicity and velocity.

Based on a study conducted by Luo et. al. at 2008, it was concluded that the pump impeller geometry has an important influence on the pump performance. This is further supported by Zhang et. al (2014), on the study of effect of pump impeller inlet on the pump efficiency. The study has varied on the pump impeller inlet dimension and observed on the impact of it on the efficiency of such pump curve. Zhang et al (2014) found that there are no direct correlation between the inlet dimension and efficiency of the pump.

Other than that, Luo et. al. (2008) also found that the blade angle will have an influence on the pump performance as well. Bacharoudis et. al. (2008) further confirmed on such claims by carrying out a study by varying the blade angle of an impeller and study on its effect on the pump performance. It was found that increasing the blade angle will decreases the pump efficiency but on the other hand increases pump head. Moreover, there is a 10% discrepancy between theoretical and predicted numerical head.

There are few fluid flow theorem that researchers have employed to simulate the unsteady flow where one of the less time and computer intensive method is Euler solution with a second-order viscosity term that were used by Hagelstein et al. (2000). However, in general other studies also finds that the Reynolds Averaged Navier-Stokes (RANS) equation shows an even better agreement between the experimental and numerical data as shown by A. Meakhail, Salem and Shafie (2014). This is because the effect of viscosity on the fluid flow pattern and pressure distribution in the pump is very significant. The effects of turbulence will also be modeled using the standard k- $\epsilon$  turbulence model that were used by A. Meakhail, Salem and Shafie (2014), Cheah, Lee and Winoto (2011) as well as Majidi and Siekmann (2000). Other than that, the log-wall function is used to resolve wall flow.

By referring to A. Meakhail, Salem and Shafie (2014) and Cheah, Lee and Winoto (2011), the “frozen rotor” simulation model are used for steady state calculation, which helps in showing the wake profile in the simulation and the “rotor/stator” model for unsteady calculation. The frozen rotor method also helps to preserve the variation of flow field across interfaces as indicated by Cheah, Lee and Winoto (2011). To further reduce the computation time, Cheah, Lee and Winoto (2011) suggested to not consider the effect of the relative change in position of the impeller and volute casing onto the change on the fluid flow. It will encourage a quick convergence of the solution. The walls of the inlet, volute and outlet will be applied with no-slip condition to include the occurrence of a secondary flow in this study.

## CHAPTER 3

### METHODOLOGY

#### 3.1 Modelling

This study utilises ANSYS turbomachinery fluid flow module to simulate the pump flow characteristics. The study was done based on an actual product to validate the accuracy of the model and then variation on the impeller inlet, outlet and blade angle parameters was carried out. The effect of such variation on the pump performance is then studied.

First, Vista CPD from ANSYS was selected to be start the blade generation. Then, the impeller option is selected. The following parameters were insert into the check box:

Table 1: Blade Specification

<b>Rotational Speed (RPM)</b>	<b>1,450</b>
<b>Volume Flow Rate (m<sup>3</sup>/hr)</b>	<b>280</b>
<b>Density (kg/m<sup>3</sup>)</b>	<b>1000</b>
<b>Head Rise (m)</b>	<b>20</b>
<b>Inlet Flow Angle (deg)</b>	<b>90</b>
<b>Merid Velocity Ratio</b>	<b>1.1</b>
<b>Blade angle (deg)</b>	<b>22.5</b>

<b>Number of Vanes</b>	<b>6</b>
------------------------	----------

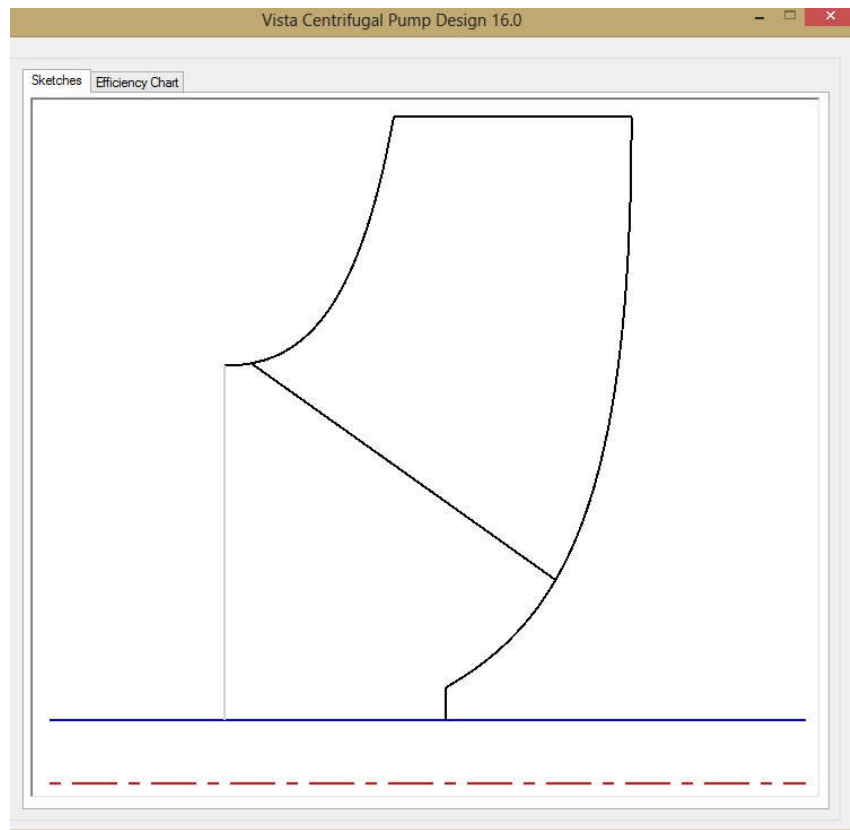


Figure 3: Vista CPD Blade Design

After that, a simple 2 dimensional view of the blade will be generated as shown in Figure 3. The pump impeller is modelled against a Grundfos pump model of KP1012-9/0. Then, the BladeGen module is used to generate the entire model of the impeller complete with the blades. In this module the outlet & inlet dimension as well as the blade angle is further adjusted. The inlet is adjusted to 170mm diameter and 97mm for the outlet. The application of BlageGen is illustrated in Figure 4. The pump impeller model is shown in Figure 5.

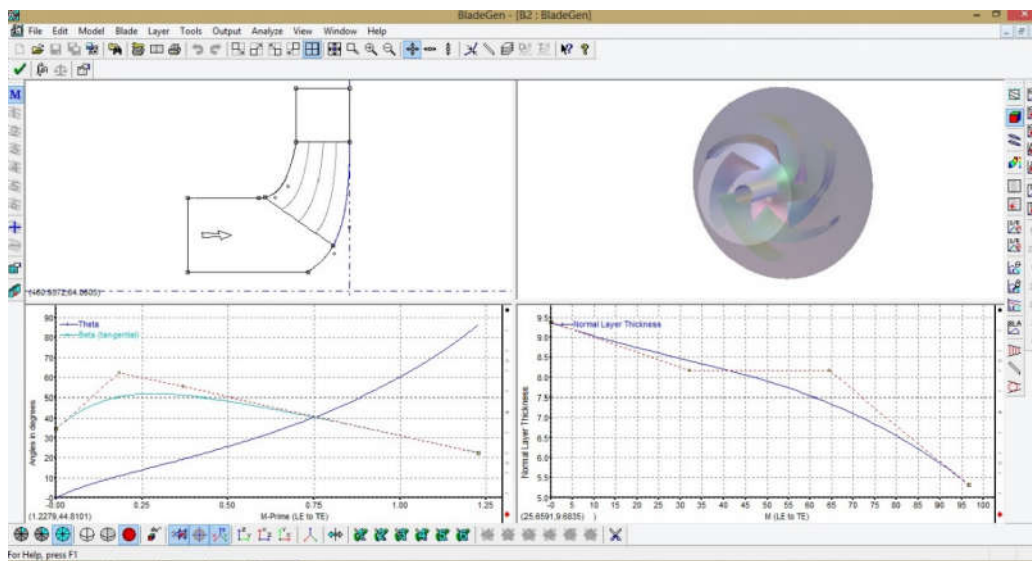


Figure 4: BladeGen

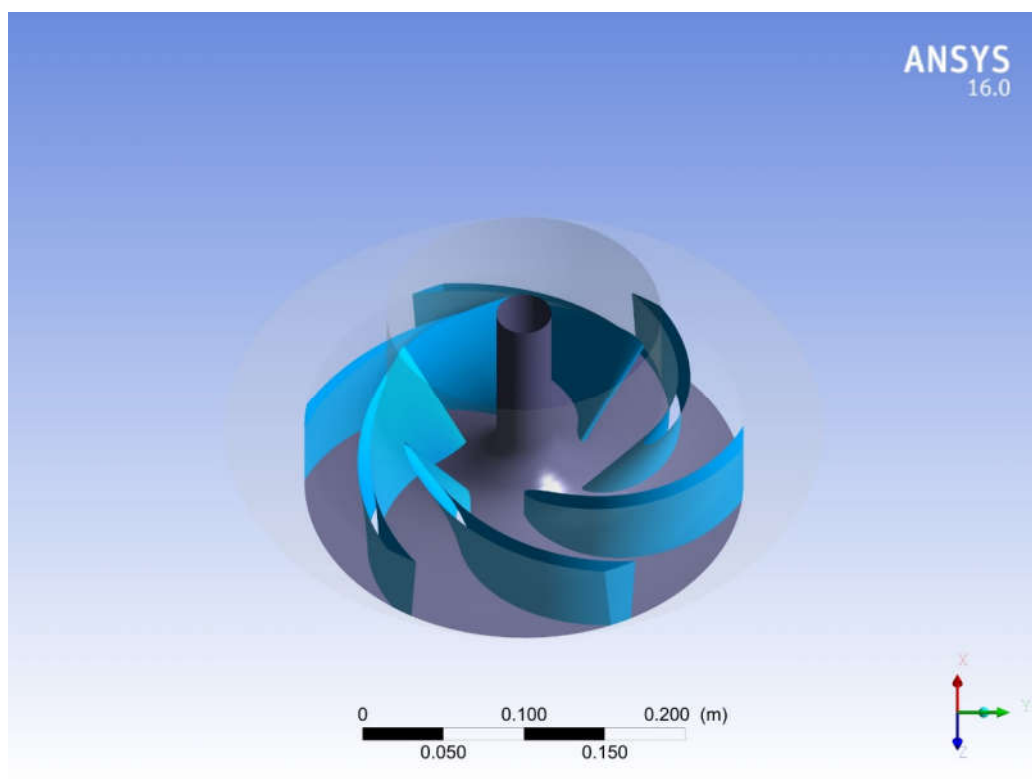


Figure 5: Pump Impeller Model

### 3.2 Meshing

Next, Turbomachinery Fluid Flow component was selected based on the method used for Kim et al, (2015). It is specifically design for bladed turbomachinery component. The mesh are automatically generated. Then, the mesh of the hub and shroud are separated to become two different entity for more precise analysis. The mesh size was globally increased to reduce the computational intensity required. The mesh quality near edge is checked.

Table 2: Mesh Information

Domain	Nodes	Elements
R1	498729	467392

Table 3: Mesh Statistics

Domain	Maximum Edge Length Ratio
R1	2494.19

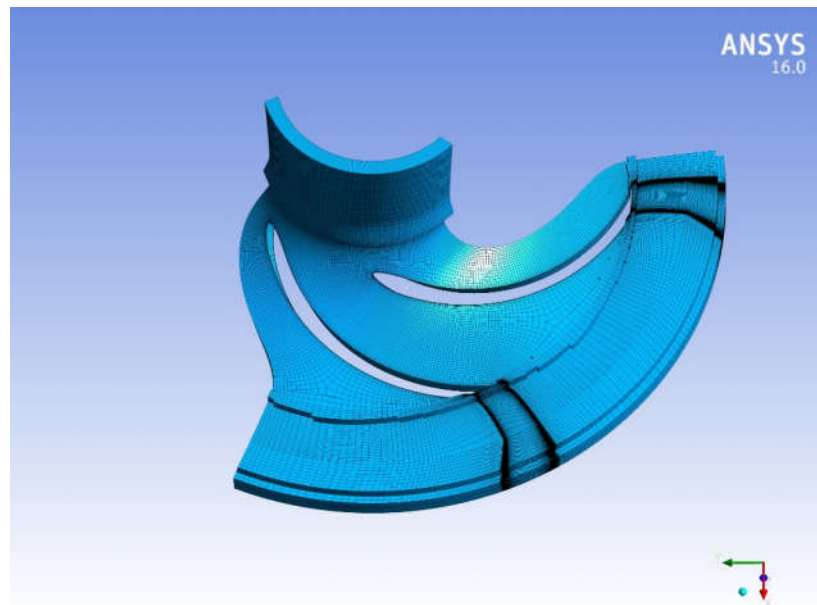


Figure 6: Meshing of Impeller

### 3.3 Setup

The turbo mode was selected to define the boundary conditions and physics. The pump option was selected to be used. Steady state flow is selected as the base model that we are using to compare is a steady flow impeller.

Next, the fluid was set as water with the turbulence flow of shear stress transport. The mass flow rate is defined. After that, the boundaries are defined. Namely, blade, hub, hub outlet, inlet, outlet and shroud.

The blades and hub are defined as no slip wall whereas the hub outlet and shroud are defined as counter rotating wall. RMS residual type of convergence method was selected and the residual target were set at  $1e^{-5}$  to ensure a refined calculation.

The head generated was set as a criteria to be monitored under the output control.

### 3.4 Solver & Results

The simulation was started when the solution module is engaged. After the convergence of solution has reached, the results were posted in the CFD-Post module and analysed. Then, a variation of mass flow rate were input to generate more data to plot out a pump curve for further analysis. The pump curve data is then tabulated and compared to the Grundfos pump curve for verification.

### 3.5 Repeat

After that, variation on the impeller specification were carried out to simulate alternative pump impeller performance. The following changes were carried out.

Alternatives 1:	Transient flow
Alternatives 2:	Reduction of inlet by 10mm
Alternatives 3:	Reduction of inlet by 20mm
Alternatives 4:	Enlargement of outlet by 10mm
Alternatives 5:	Enlargement of outlet by 20mm
Alternatives 6:	Reduction in blade angle by 2.5°

The results are then tabulated and analysed.

## CHAPTER 4

### RESULTS AND DISCUSSION

#### 4.1 Base Model

Table 4: Pump Curve Data for Base Pump

	<b>Volumetric Flow Rate</b>	<b>Head</b>	<b>Total Efficiency</b>
<b>Units</b>	<b>m<sup>3</sup>/hr</b>	<b>m</b>	<b>%</b>
<b>DP 1</b>	280	22.25	94.74
<b>DP 2</b>	360	19.26	95.69
<b>DP 3</b>	468	15.15	95.39
<b>DP 4</b>	540	12.37	94.40
<b>DP 5</b>	630	8.76	90.64
<b>DP 6</b>	720	4.56	75.47
<b>DP 7</b>	810	0.41	16.86

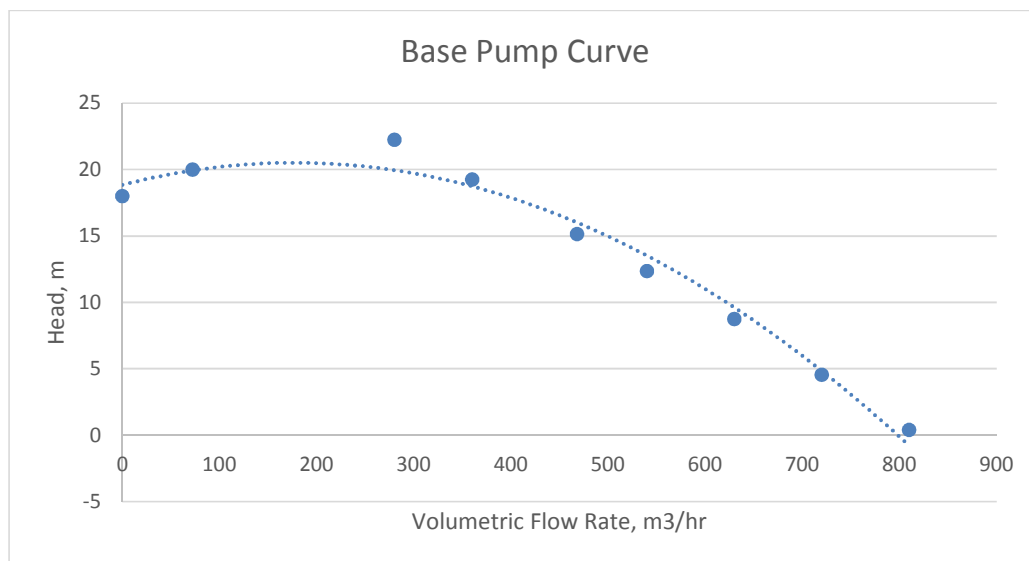


Figure 7: Base Pump Curve

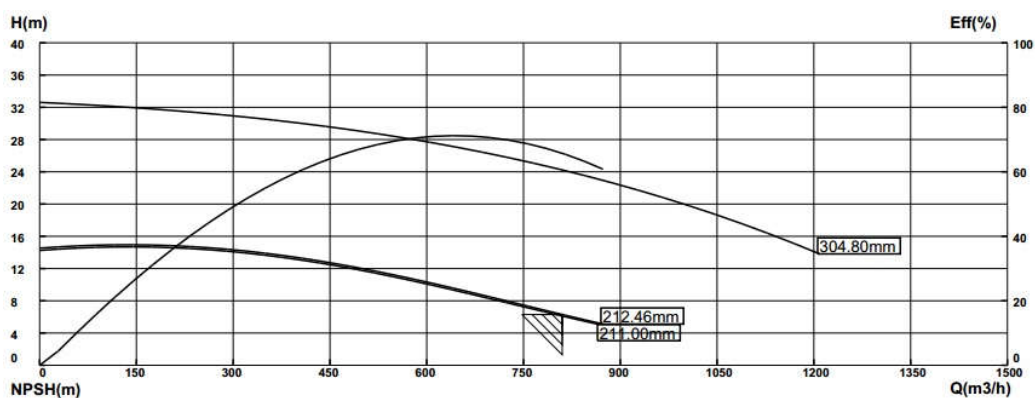


Figure 8: Grundfos Pump Curve

Figure 7 is the theoretical base pump curve that were obtained from the simulation itself whereas the pump curve in Figure 8 is the Grundfos pump curve. By comparing both chart, we can observe that both are having a similar curve of performance. However, the pump curve simulated has a relatively higher pump head than the actual product itself. This is due to the loss of energy through friction and heat in an actual pumpset. Thus, it can be concluded that the simulation model is similar to the actual product and able to be used in further analysis.

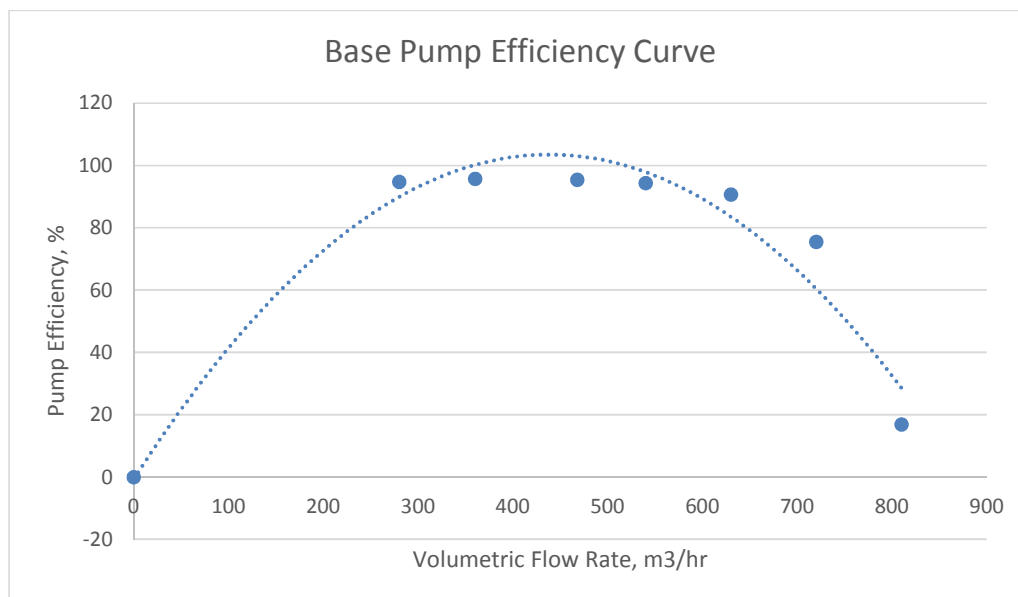


Figure 9: Base Pump Efficiency Curve

The efficiency achieved by the simulation is exceeding 100% at certain points due to the totally ideal environmental performance and condition. In real product it is still impossible to achieve a 100% efficiency. Another reason that the efficiency of the simulated pump is way higher than the original product is because the simulation does not include the volute in the simulation. Hence, eliminating a major energy loss of the pump.

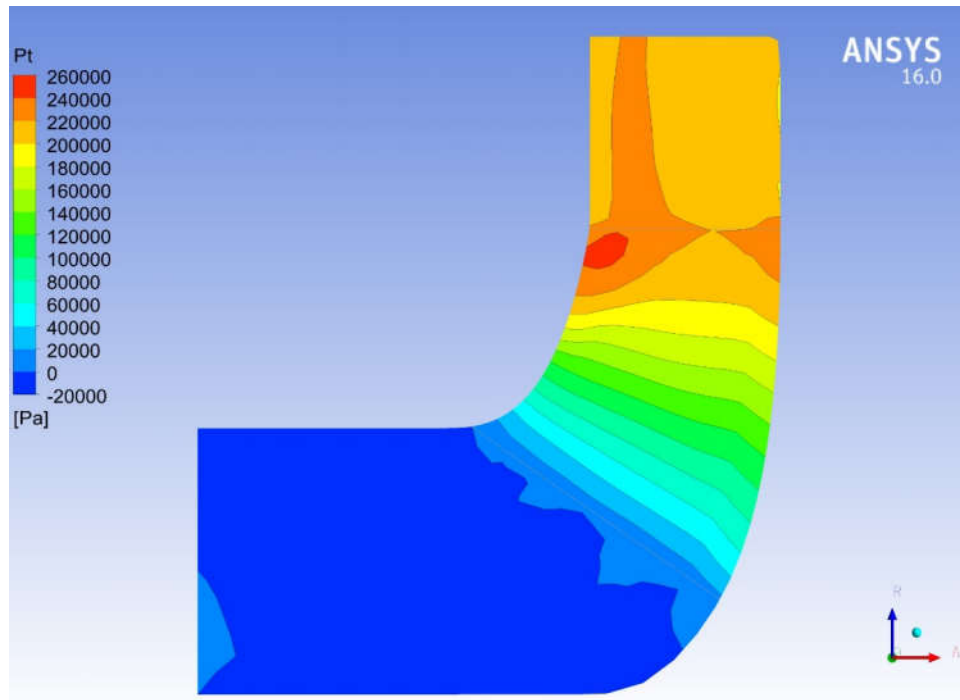


Figure 10: Total pressure contour of the fluid in the impeller

By referring to Figure 10, we can observe the total pressure distribution contour in the impeller. At the inlet there is a negative suction low pressure zone and a high pressure discharge at the outlet. The pressure increases as it travels from inlet to outlet. However, there is an even higher concentrated pressure zone near the edge of the pump impeller blade.

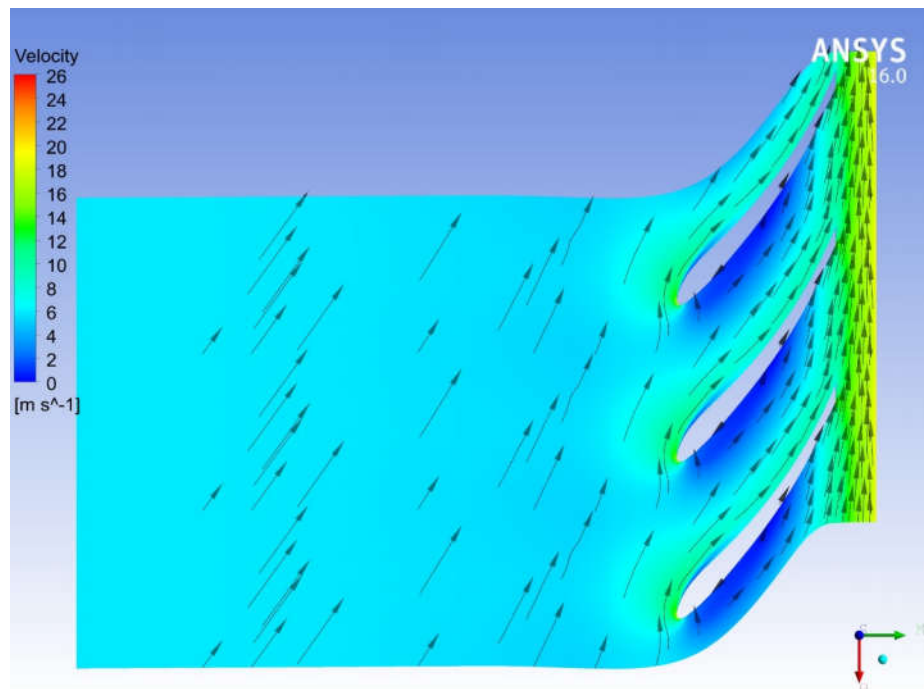


Figure 11: Velocity distribution at 20% span

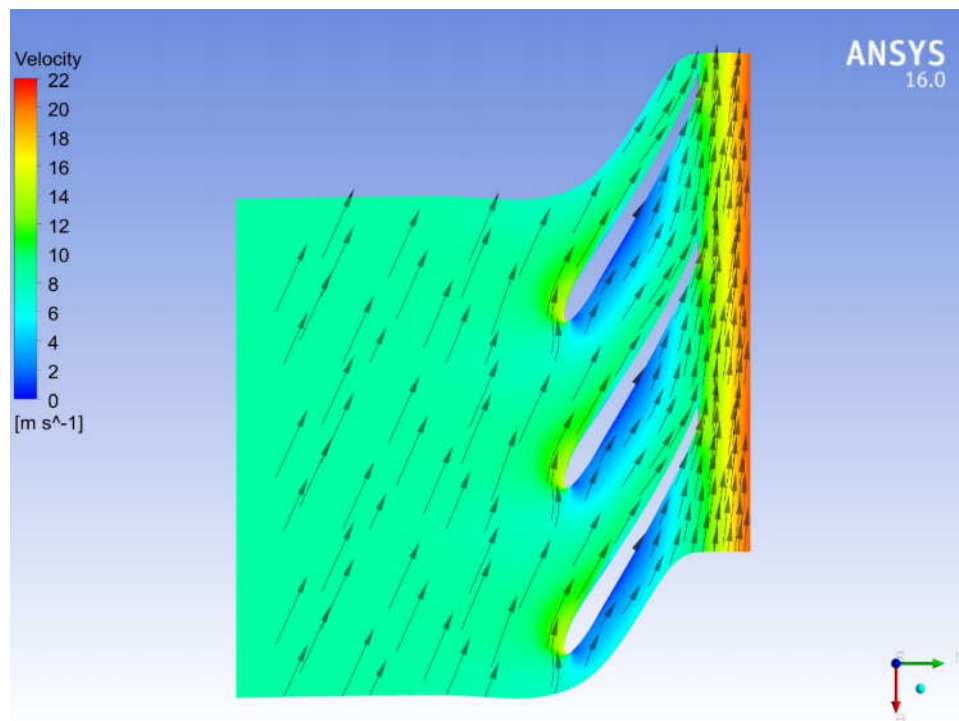


Figure 12: Velocity distribution at 50% span

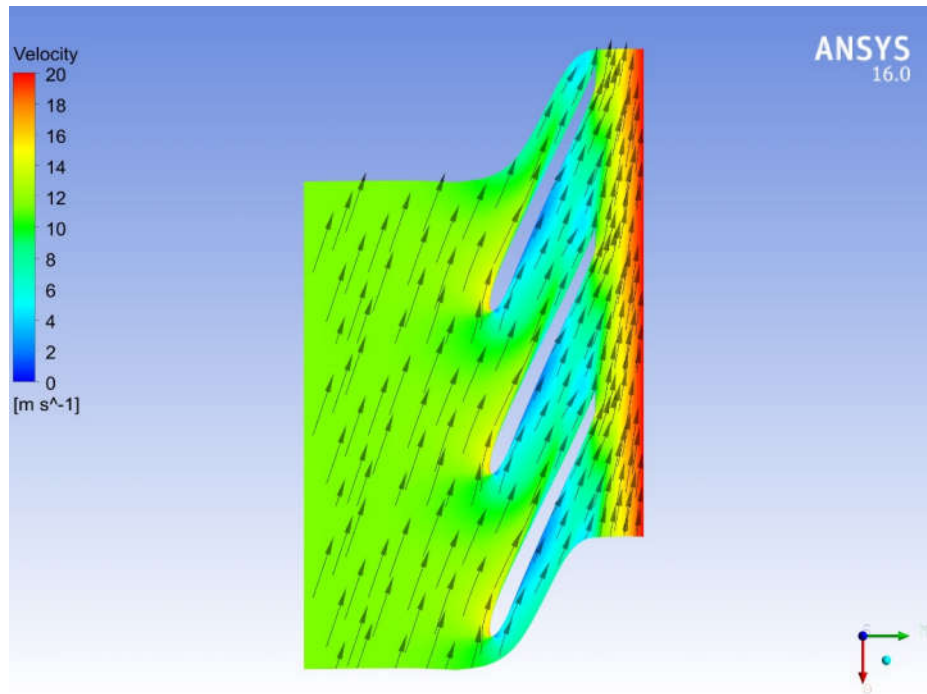


Figure 13: Velocity distribution at 80% span

Figure 11 shows the velocity distribution at 20% span of the blade. It can be observed that the flow is relatively slower on the inlet side and higher on the discharge direction. The flow above the blade has a relatively higher velocity than the other side of the blade. On Figure 12 and 13 the velocity contour can be noticed that it has relatively increased. The contour of velocity difference on both sides of the blades has reduced in area indicating the higher flow. The maximum velocity is recorded near the wall of the shroud.

## 4.2 Transient Model

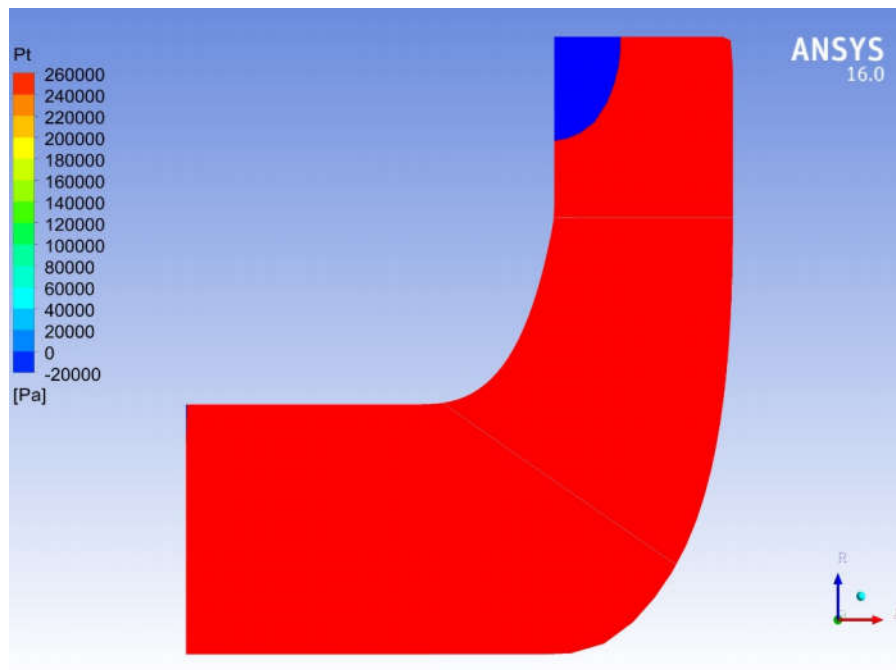


Figure 14: Total pressure contour of the fluid in the impeller

In the transient model the total pressure is shown in Figure 14. The pressure distribution does not match the base pump pressure contour pattern where the inlet has a negative suction flow and high pressure discharge. The pressure distribution in the transient model is not acceptable and it is caused by wrong input in the simulation.

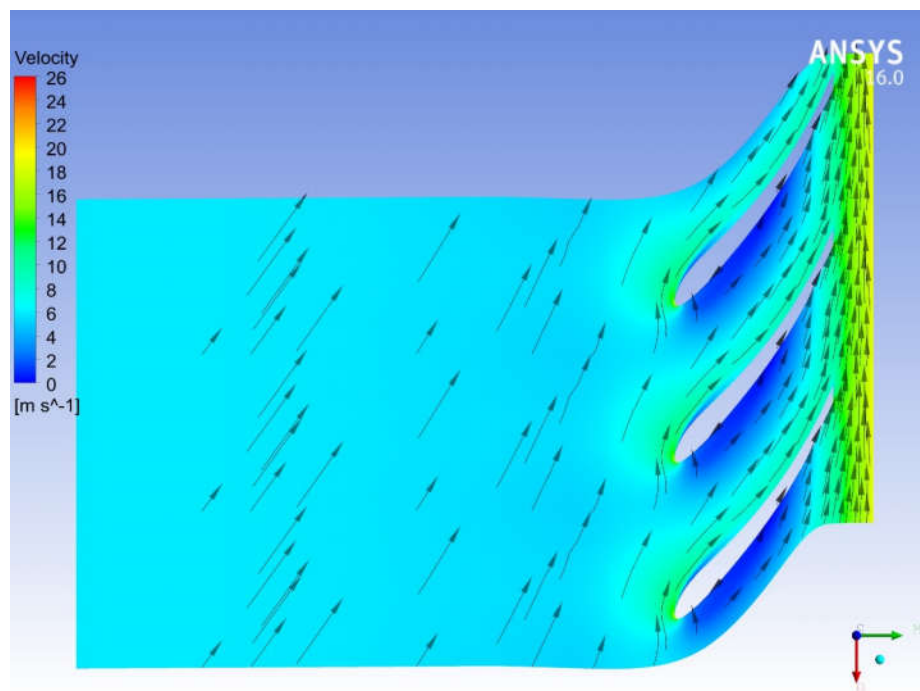


Figure 15: Velocity distribution at 20% span

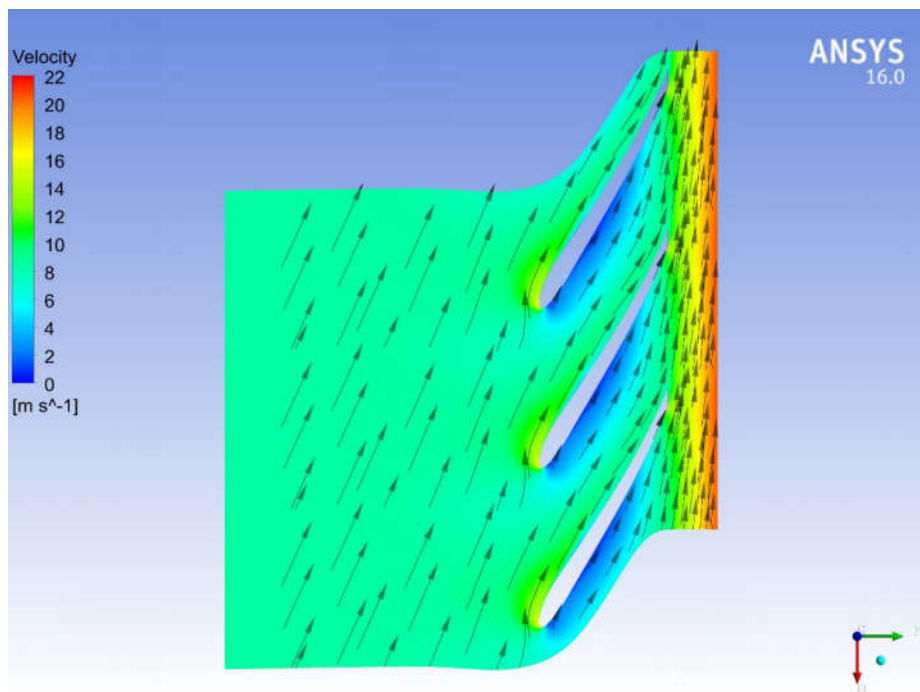


Figure 16: Velocity distribution at 50% span

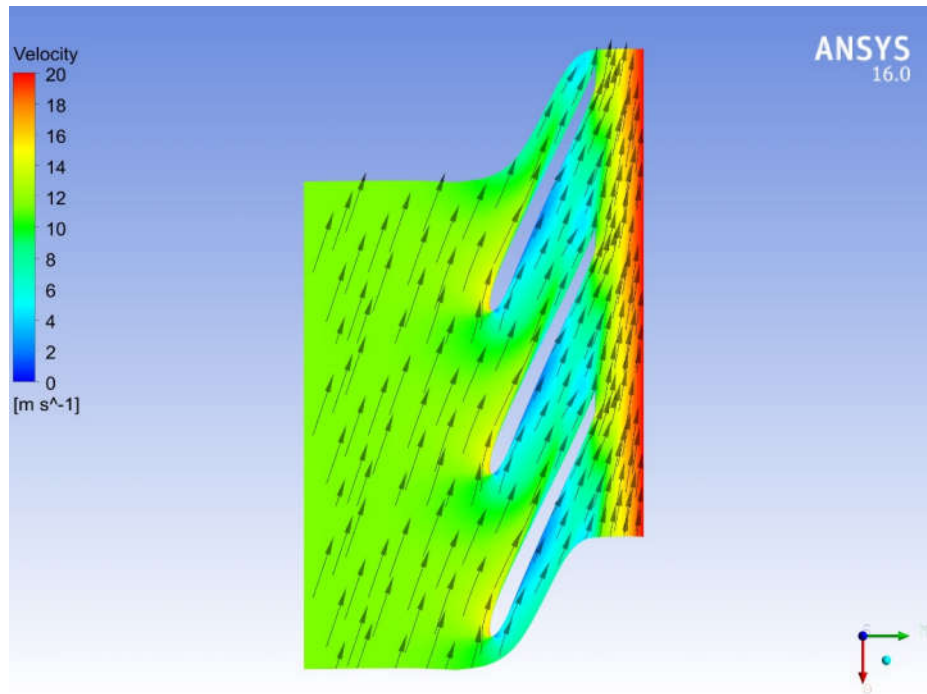


Figure 17: Velocity distribution at 80% span

Comparing Figure 15-17 to the base model velocity distribution contour, there are no differences observed. It has an identical velocity profile at both sides of the blades as well.

### 4.3 Reduction of Inlet

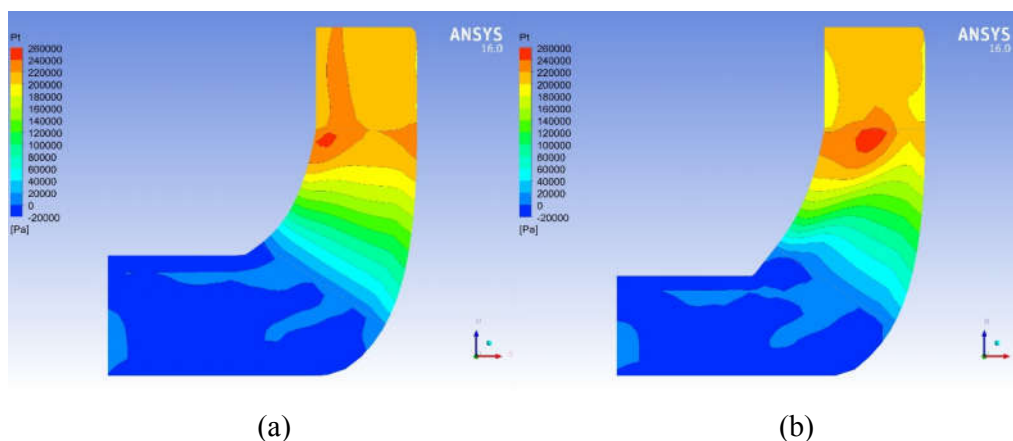


Figure 18: Total pressure distribution in reduced inlet 10mm(a) and reduced inlet 20mm(b)

As the inlet dimension is reduced, the pressure distribution at the inlet became un-uniform. There are higher pressure flow observed at the inlet area that are not evenly distributed. This could indicate an unsteady flow. The high pressure zone observed in the base pump shifts towards the center of the outlet discharge as the inlet dimension decreases. Referring to Figure 18 (b), the pressure distribution contour is distorted and uneven. Low pressure pockets are observed near the walls of the discharge outlet for Figure 18 (b).

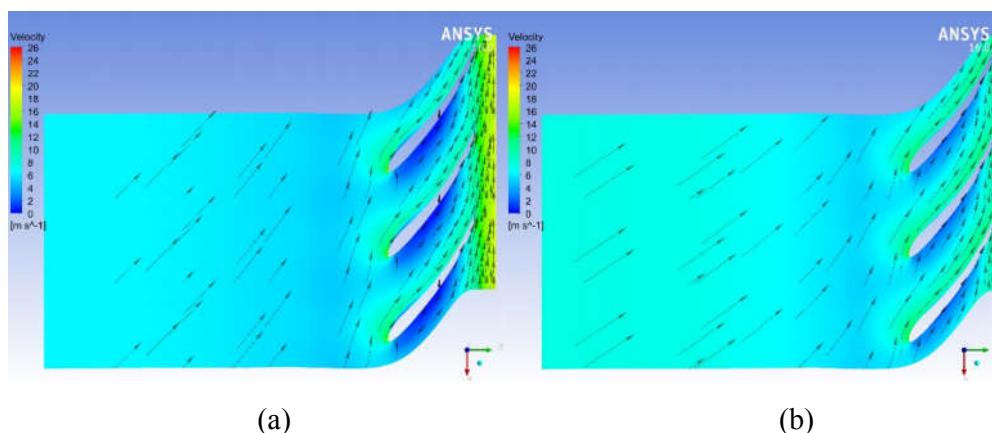
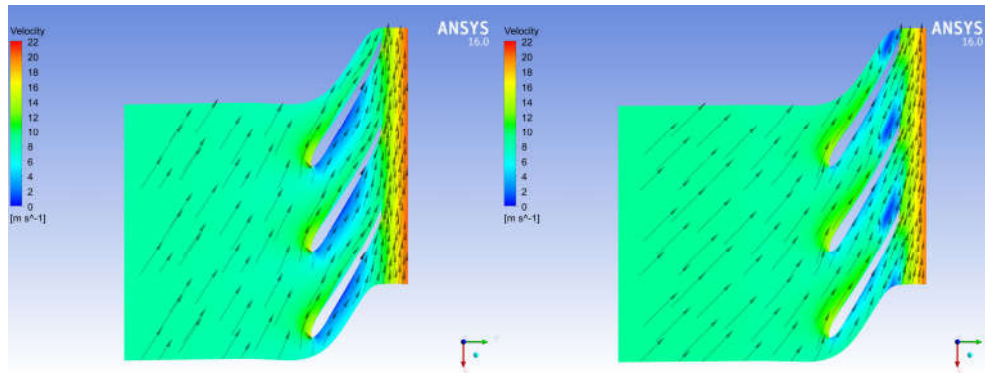


Figure 19: Velocity distribution at 20% span for reduced inlet 10mm(a) & reduced inlet 20mm(b)

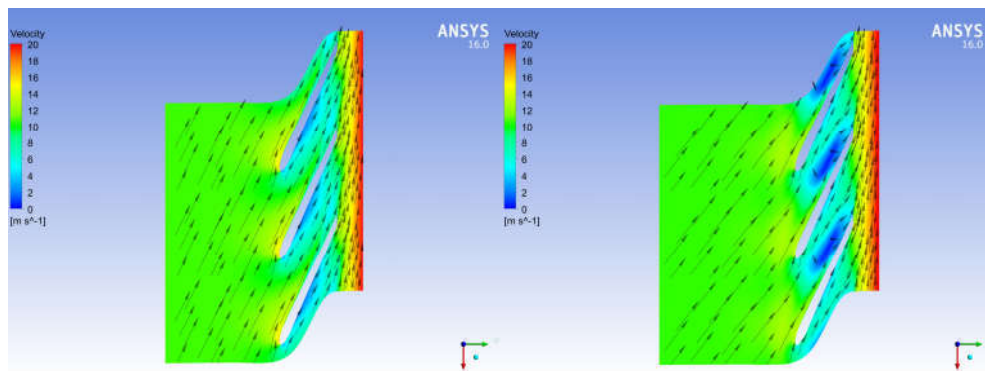
Referring to Figure 19, as the inlet dimension reduces, the velocity at the inlet increases. The velocity profile at both sides of the blade increases as the inlet dimension reduces. However, it can be observed that the velocity difference of inlet and outlet of the reduced inlet pump is lower.



(a)

(b)

Figure 20: Velocity distribution at 50% span for reduced inlet 10mm(a) & reduced inlet 20mm(b)



(a)

(b)

Figure 21: Velocity distribution at 80% span for reduced inlet 10mm(a) & reduced inlet 20mm(b)

Figure 21 (a) shows a flow that is similar to the base pump but with a higher velocity distribution. On the other hand, the flow near the trailing edge of the blade has low flow region possibly caused by secondary flow. The fluid flow in Figure 21 (a) has a similar contour to the base pump whereas the fluid flow pattern in Figure 21 (b) has developed a low flow turbulent region.

Table 5: Pump curve data for reduced 10mm pump

	<b>Volumetric Flow Rate</b>	<b>Head</b>	<b>Total Efficiency</b>
<b>Units</b>	<b>m<sup>3</sup>/hr</b>	<b>m</b>	<b>%</b>
<b>DP 1</b>	180	24.70	84.58
<b>DP 2</b>	280	22.23	94.59
<b>DP 3</b>	360	19.08	95.12
<b>DP 4</b>	468	14.89	94.31
<b>DP 5</b>	540	12.05	92.49
<b>DP 6</b>	630	8.42	88.20
<b>DP 7</b>	720	4.80	77.34
<b>DP 8</b>	810	1.01	35.28

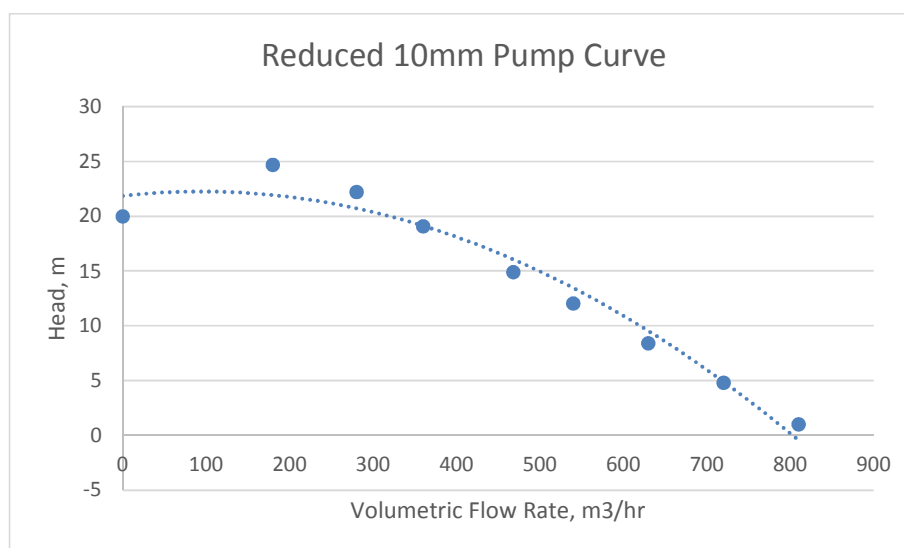


Figure 22: Reduced 10mm Pump Curve

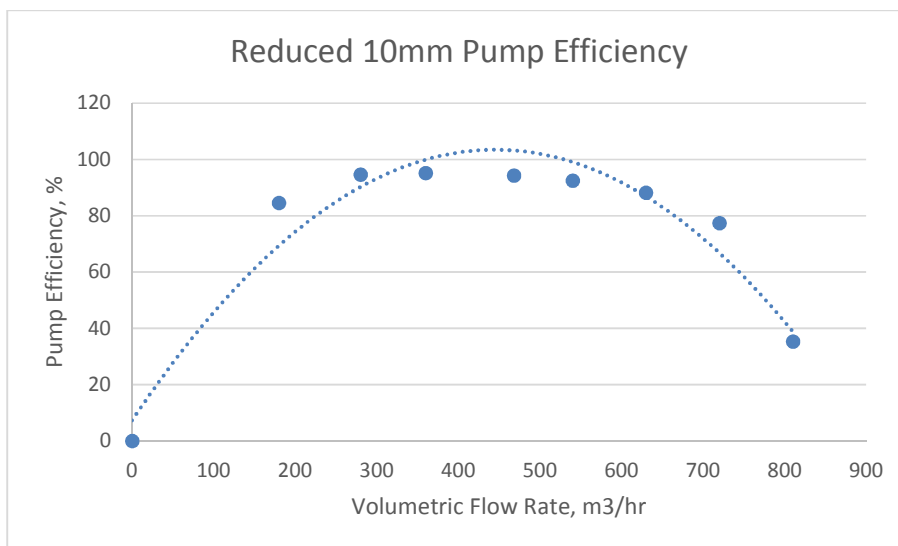


Figure 23: Reduced 10mm Pump Efficiency

Based on Figure 22, we can observe that the pump head generated is generally lower than the base pump but the curve appear to be even flatter, which increases the area of the best efficiency point. The pump efficiency curve shown on Figure 23 indicates that the pump efficiency at the pump duty point, 500m<sup>3</sup>/hr onwards has a slightly higher pump efficiency.

Table 6: Pump curve data for reduced 20mm pump

	<b>Volumetric Flow Rate</b>	<b>Head</b>	<b>Total Efficiency</b>
<b>Units</b>	<b>m<sup>3</sup>/hr</b>	<b>m</b>	<b>%</b>
<b>DP 1</b>	280	21.66	90.52
<b>DP 2</b>	360	18.47	90.43
<b>DP 3</b>	468	13.52	87.98
<b>DP 4</b>	540	10.11	83.30
<b>DP 5</b>	630	5.82	68.31
<b>DP 6</b>	720	1.29	25.33

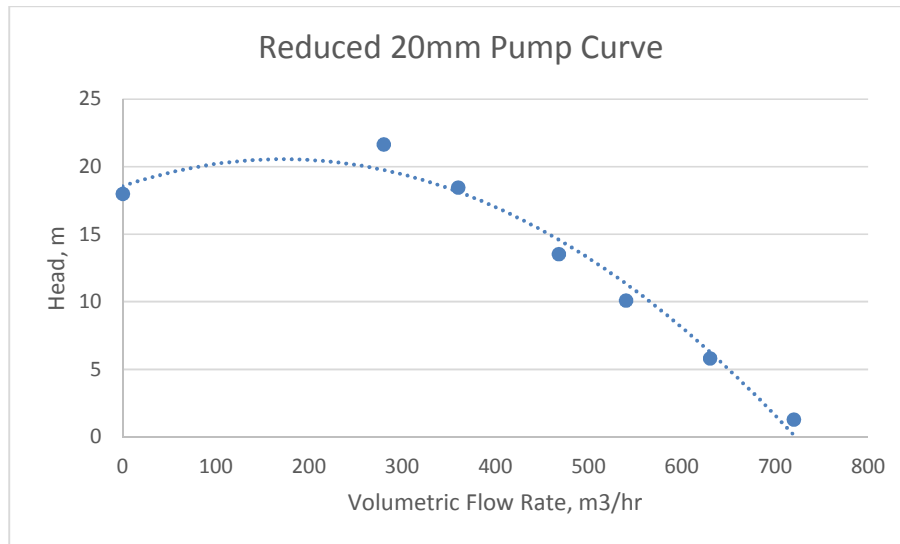


Figure 24: Reduced 20mm Pump Curve

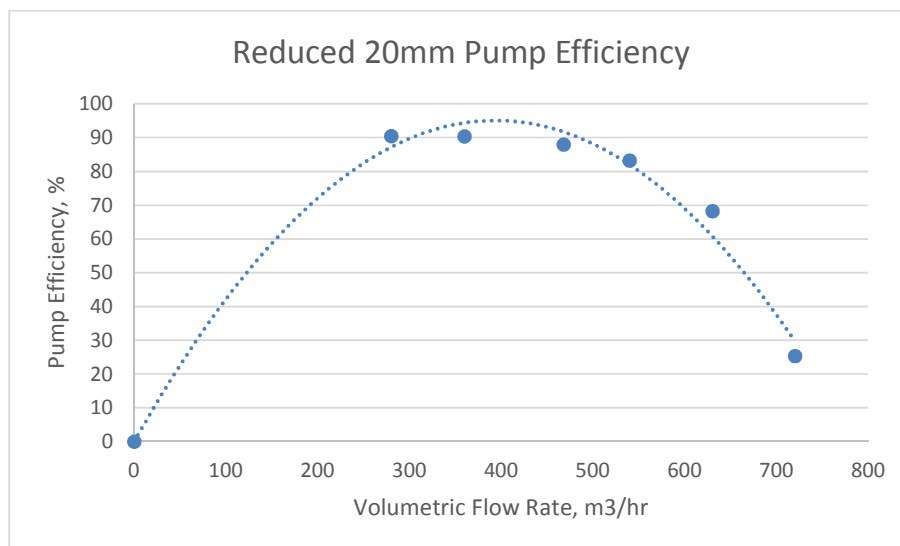


Figure 25: Reduced 20mm Pump Efficiency

The pump curve generated by the reduced 20mm pump is relatively lower than the base pump in terms of pump head generated as shown in Figure 24. Moreover, it has a relatively sharper drop near the end of the curve. Hence, lowering the area of BEP. Other than that, the pump efficiency curve indicated in Figure 25 shows that the pump efficiency has in general dropped all across the curve.

#### 4.4 Enlargement of outlet

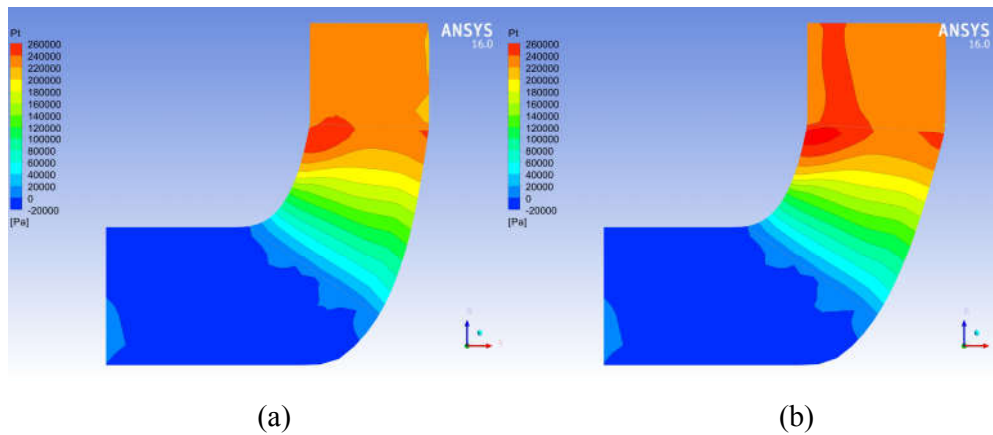


Figure 26: Total pressure distribution for enlarged outlet 10mm(a) & enlarged outlet 20mm

One of the main sign that can be picked up through observation is the increase in pressure in the outlet region where in Figure 26 (a) the entire outlet region has increase in pressure and the high pressure (indicated in red) has increased in area. Other than that, the pump in Figure 26 (b) shows an even higher pressure increase on the outlet region where the high pressure zone (indicated in red) has further enlarged. The pressure distribution on the inlet and blade region however has remain similar to the base pump.

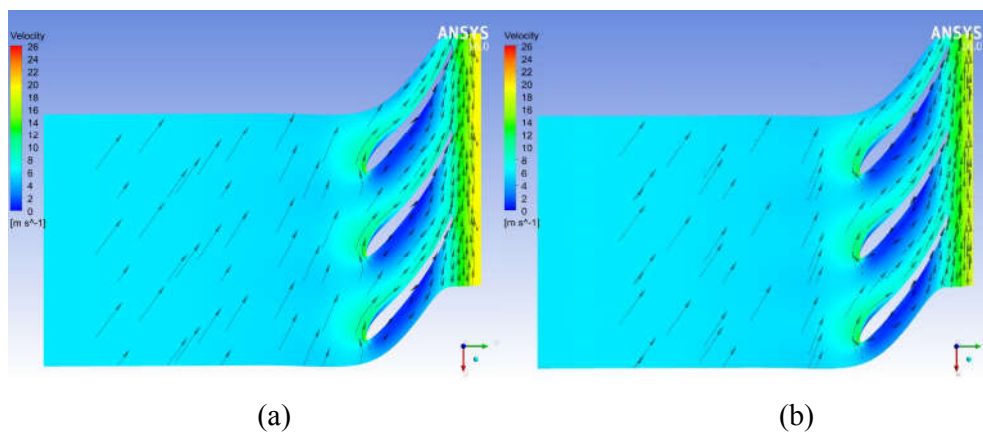
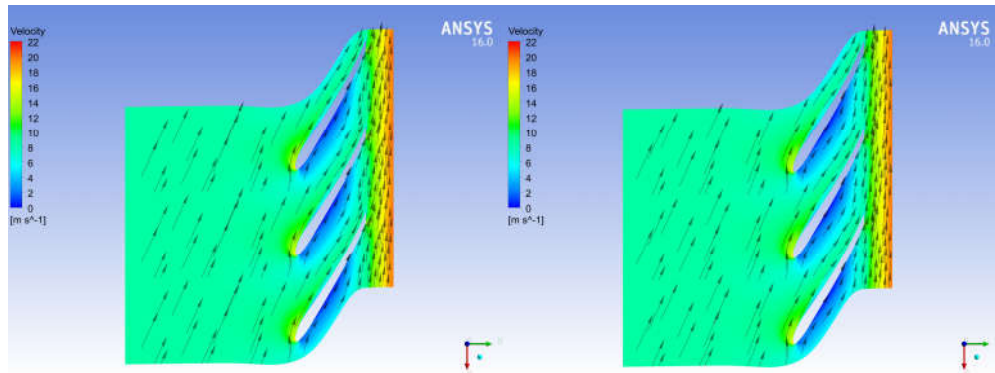


Figure 27: Velocity distribution at 20% span for enlarged outlet 10mm(a) & enlarged outlet 20mm

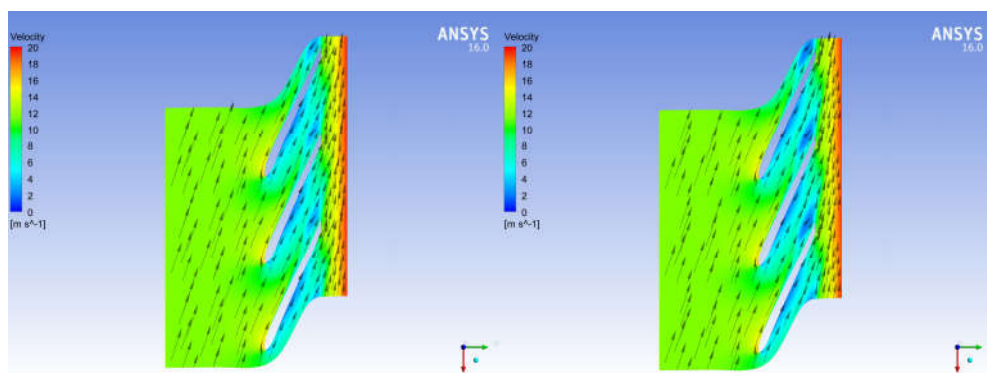
Figure 27 shows that the fluid flow near the leading edge of the blade has a slower flow than the base pump and it is especially obvious in Figure 27 (b). A minor development of reverse flow can be observed in both images shown in Figure 27 on the bottom of the blade.



(a) (b)

Figure 28: Velocity distribution at 50% span for enlarged outlet 10mm(a) & enlarged outlet 20mm(b)

By comparison, the slow flow region (indicated in dark blue) in Figure 28 are relatively thinner than the base pump. Furthermore, the flow in between the trailing edge of the blades appear to curve into the opposite direction of the flow. This is especially noticeable in Figure 28 (a). The situation is less severe in Figure 28 (b).



(a) (b)

Figure 29: Velocity distribution at 80% span for enlarged outlet 10mm(a) & enlarged outlet 20mm(b)

In Figure 29, we can observe that a secondary flow is starting to develop as there are slow flow region present on the trailing edge of the blades. The slow flow region is indicated with blue in colour. The effect is even more significant in the 20mm reduced outlet pump set.

Table 7: Pump curve data for enlarged 10mm pump

	<b>Volumetric Flow Rate</b>	<b>Head</b>	<b>Total Efficiency</b>
<b>Units</b>	<b>m<sup>3</sup>/hr</b>	<b>m</b>	<b>%</b>
<b>DP 1</b>	180	24.50	83.70
<b>DP 2</b>	280	23.60	94.61
<b>DP 3</b>	360	20.90	95.98
<b>DP 4</b>	468	17.29	96.02
<b>DP 5</b>	540	14.90	95.45
<b>DP 6</b>	630	11.59	92.18
<b>DP 7</b>	720	7.85	83.98
<b>DP 8</b>	810	3.88	64.92

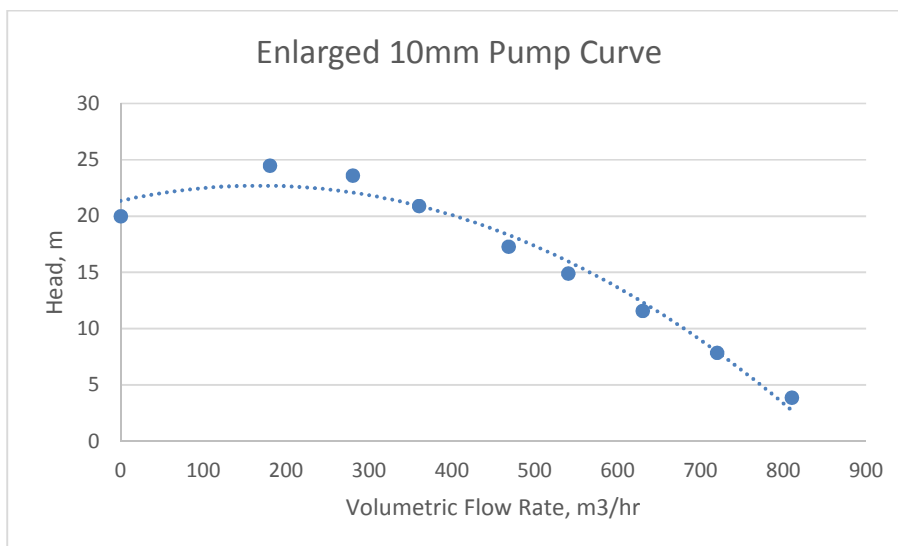


Figure 30: Enlarged 10mm pump curve

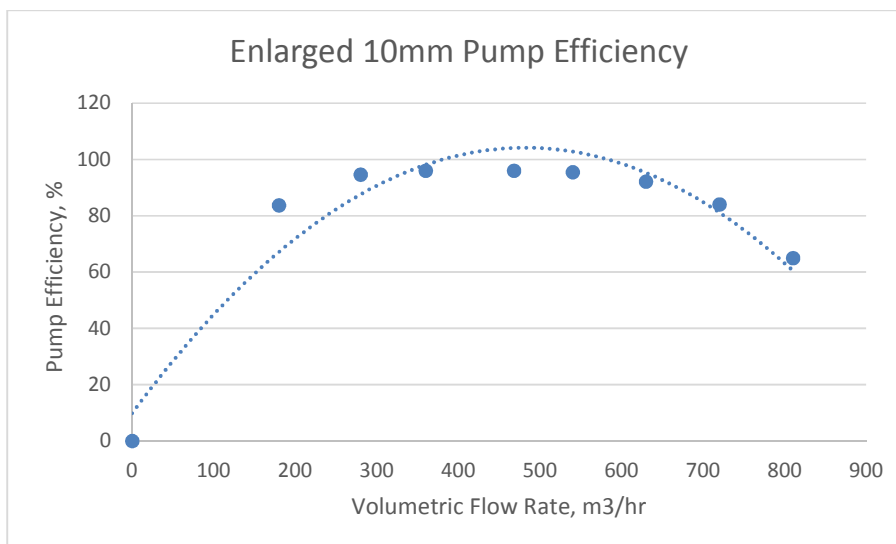


Figure 31: Enlarged 10mm pump efficiency

In general, the pump head produced through the enlargement of outlet is higher than the base pump. This is indicated in Figure 30. In terms of BEP, the pump curve has a flatter curve and thus higher BEP area. The pump efficiency of the pump are also slightly higher than the base pump.

Table 8: Pump curve data for enlarged 20mm pump

	<b>Volumetric Flow Rate</b>	<b>Head</b>	<b>Total Efficiency</b>
<b>Units</b>	<b>m<sup>3</sup>/hr</b>	<b>m</b>	<b>%</b>
<b>DP 1</b>	280	24.33	94.40
<b>DP 2</b>	360	21.86	96.13
<b>DP 3</b>	468	18.54	96.33
<b>DP 4</b>	540	16.31	95.81
<b>DP 5</b>	630	13.30	93.06
<b>DP 6</b>	720	9.88	86.78
<b>DP 7</b>	810	6.19	74.53
<b>DP 8</b>	900	2.63	49.77

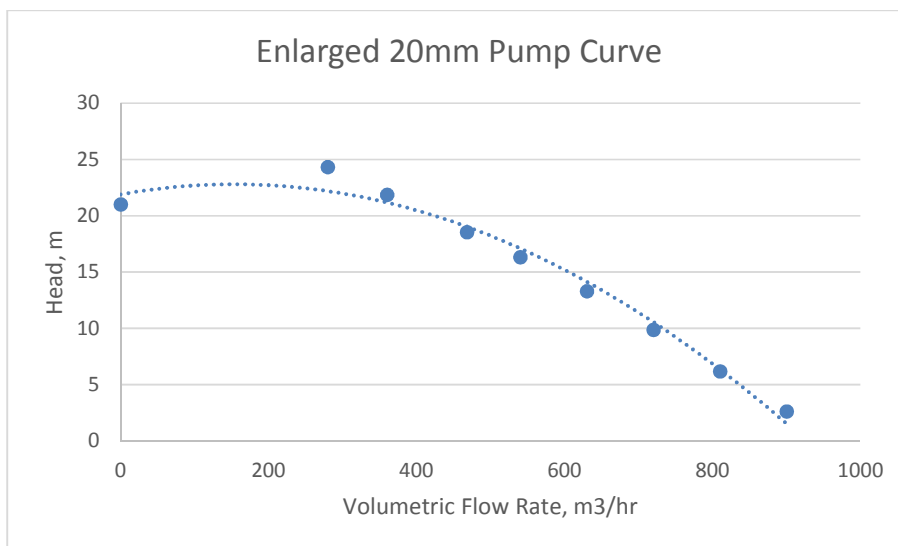


Figure 32: Enlarged 20mm Pump Curve

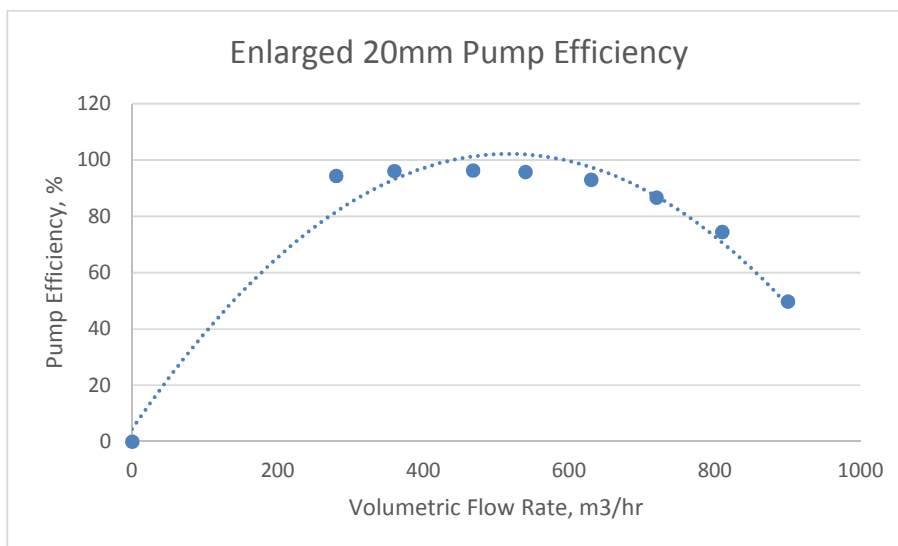


Figure 33: Enlarged 20mm pump efficiency

The pump curve produced in Figure 32 has a relatively higher head generated than the base pump curve. Moreover, it has a flatter curve towards the end of the chart. Thus, the BEP area is larger than the base pump. The pump efficiency curve in general are slightly higher than the base pump as illustrated in Figure 33.

## 4.5 Reduced Blade Angle

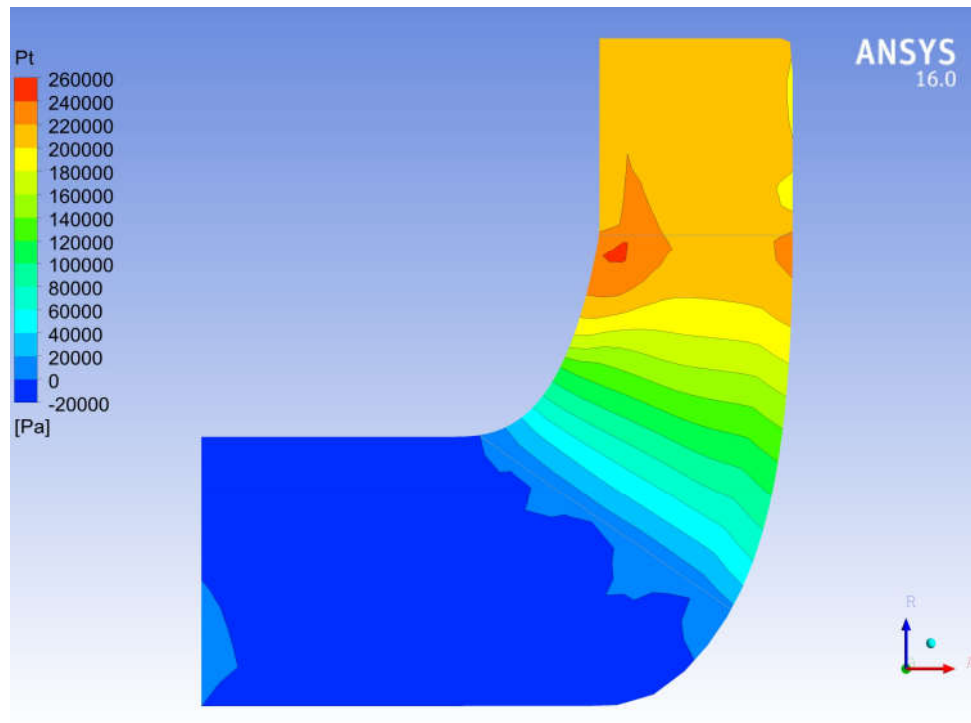


Figure 34: Total pressure contour of the fluid in the impeller

One of the most significant difference that can be observed from the pressure contour image shown in Figure 34 is the low pressure region at the outlet region of the impeller. It is noticeable that the high pressure region (indicated in red) has decrease in size compared to the base model. Other than that, both have a similar pressure contour across the inlet region as well as the blade region.

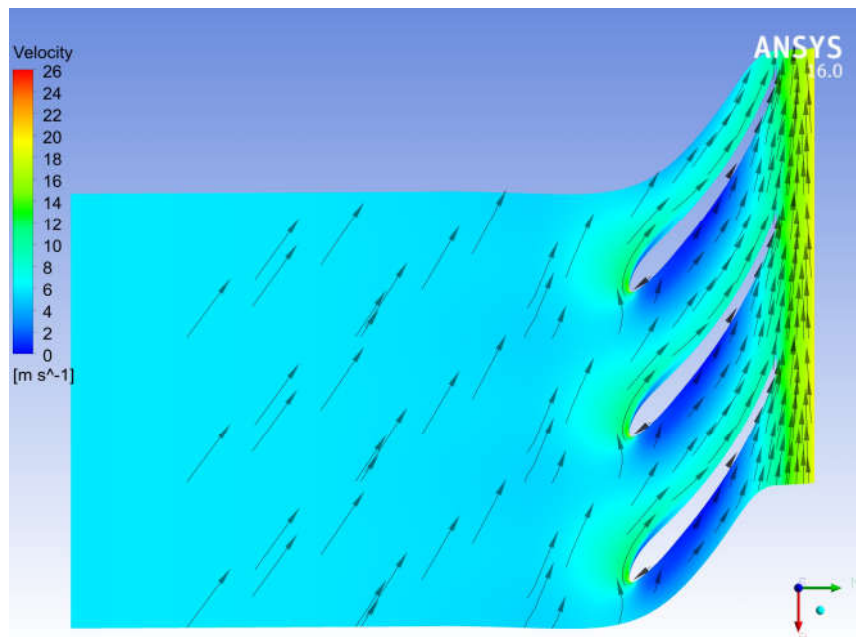


Figure 35: Velocity distribution at 20% span

It can be observed that the flow of fluid at the trailing edge of the blade are more uniform than the base model where the fluid flows straight towards the outlet without any distortion. The flow on the bottom of the blade is relatively faster as shown in Figure 35.

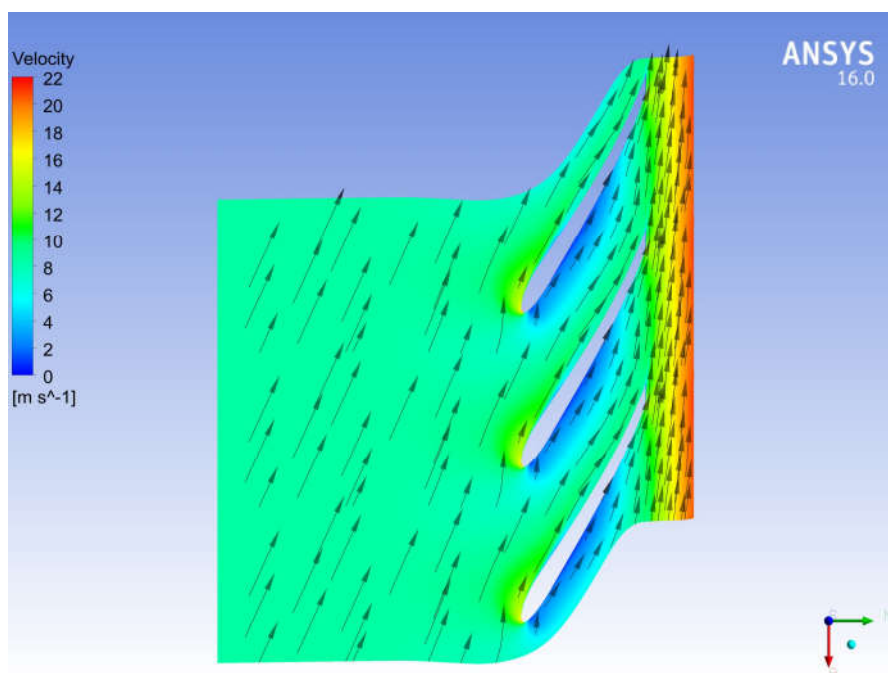


Figure 36: Velocity distribution at 50% span

One of the main difference that is noticeable is the low flow region at the bottom of the blade of current pump impeller (as illustrated in Figure 36) has a smoother flow than the base pump. In the base pump there appears to be a slight bump where the fluid will not flow in a straight line.

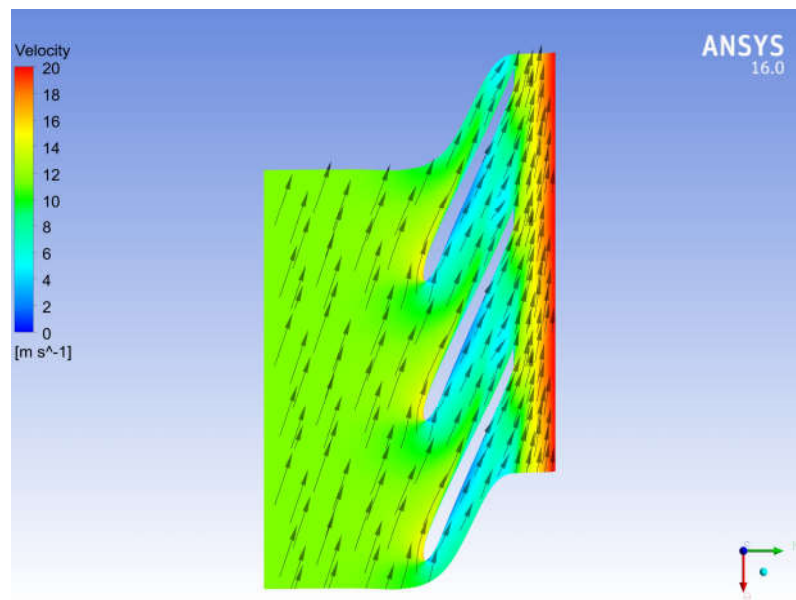


Figure 37: Velocity distribution at 80% span

The velocity vector at the edge of the trailing edge in Figure 37 has slight distortion compared to the base pump. Other than that, it has a similar velocity vector distribution as the base model.

## CHAPTER 5

### CONCLUSION AND RECOMMENDATIONS

#### 5.1 Conclusion

As a conclusion, running a pump beyond its operating point or design point is not recommended as it induces turbulent flow within the pump itself and causes problems that are visible in the data generated for the transient flow.

Furthermore, by decreasing the inlet by 10mm a better impeller performance can be achieved with higher pump efficiency by 2% and flatter pump curve generated. With flatter pump curve a larger BEP area can be achieved. However, further decreasing the pump inlet will cause a drop in pump performances.

Through the enlargement of the outlet a better pump performance in terms of pump head and efficiency can be achieved. However, due to the development of secondary flow observed, it will eventually cause vibration and affect the mechanical parts.

Reduction in the blade angle will benefit the fluid flow in the impeller with a smoother flow and more uniform velocity distribution.

##### 5.1.1 Recommendation

Hence, it is recommended that a slight reduction in pump inlet dimension by 10mm to be carried out to achieve a flatter pump curve with a larger operating range for the pump. Other than that, the angle of blade can be reduced by  $2.5^\circ$  to achieve a smoother flow in the impeller and better pump performance.

## REFERENCES

- A. Meakhail, T., Salem, M. and Shafie, I. (2014). Steady and Unsteady Flow inside a Centrifugal Pump for Two Different Impellers. *International Journal of Energy and Power Engineering*, 3(2), p.65.
- Ayder, E., Van den Braembussche, R. and Brasz, J. (1993). Experimental and Theoretical Analysis of the Flow in a Centrifugal Compressor Volute. *J. Turbomach.*, 115(3), p.582.
- Bacharoudis, E., Filios, A., Mentzos, M. and Margaritis, D. (2008). Parametric Study of a Centrifugal Pump Impeller by Varying the Outlet Blade Angle. *The Open Mechanical Engineering Journal*, 2(1), pp.75-83.
- Barrio, R., Parrondo, J. and Blanco, E. (2010). Numerical analysis of the unsteady flow in the near-tongue region in a volute-type centrifugal pump for different operating points. *Computers & Fluids*, 39(5), pp.859-870.
- Chakraborty, S. and Pandey, K. (2011). Numerical Studies on Effects of Blade Number Variations on Performance of Centrifugal Pumps at 4000 RPM. *IJET*, 3(4), pp.410-416.
- Cheah, K., Lee, T. and Winoto, S. (2011). Numerical Study of Inlet and Impeller Flow Structures in Centrifugal Pump at Design and Off-design Points. *International Journal of Fluid Machinery and Systems*, 4(1), pp.25-32.
- Cheah, K., Lee, T. and Winoto, S. (2011). Unsteady Analysis of Impeller-Volute Interaction in Centrifugal Pump. *International Journal of Fluid Machinery and Systems*, 4(3), pp.349-359.
- CROBA, D. and KUENY, J. (1996). NUMERICAL CALCULATION OF 2D, UNSTEADY FLOW IN CENTRIFUGAL PUMPS: IMPELLER AND VOLUTE INTERACTION. *International Journal for Numerical Methods in Fluids*, 22(6), pp.467-481.
- Dong, R., Chu, S. and Katz, J. (1997). Effect of Modification to Tongue and Impeller Geometry on Unsteady Flow, Pressure Fluctuations, and Noise in a Centrifugal Pump. *J. Turbomach.*, 119(3), p.506.
- González, J. and Santolaria, C. (2006). Unsteady Flow Structure and Global Variables in a Centrifugal Pump. *Journal of Fluids Engineering*, 128(5), p.937.

- Hagelstein, D., Hillewaert, K., Van den Braembussche, R., Engeda, A., Keiper, R. and Rautenberg, M. (2000). Experimental and Numerical Investigation of the Flow in a Centrifugal Compressor Volute. *J. Turbomach.*, 122(1), p.22.
- Henshaw, T. (2015). [image] Available at: <http://www.pump-zone.com/sites/default/files/Axial%20Thrust%20-%20Fig.%201%20-%20Horiz.%20Pump%20no%20caption.jpg> [Accessed 3 Sep. 2015].
- Kaupert, K. and Staubli, T. (1999). The Unsteady Pressure Field in a High Specific Speed Centrifugal Pump Impeller—Part I: Influence of the Volute. *Journal of Fluids Engineering*, 121(3), p.621.
- Kim, J., Oh, K., Pyun, K., Kim, C., Choi, Y. and Yoon, J. (2012). Design optimization of a centrifugal pump impeller and volute using computational fluid dynamics. *IOP Conf. Ser.: Earth Environ. Sci.*, 15(3), p.032025.
- Luo, X., Zhang, Y., Peng, J., Xu, H. and Yu, W. (2008). Impeller inlet geometry effect on performance improvement for centrifugal pumps. *Journal of Mechanical Science and Technology*, 22(10), pp.1971-1976.
- Majidi, K. and Siekmann, H. (2000). Numerical Calculation of Secondary Flow in Pump Volute and Circular Casings using 3D Viscous Flow Techniques. *International Journal of Rotating Machinery*, 6(4), pp.245-252.
- Moffatt, H. (2014). Helicity and singular structures in fluid dynamics. *Proceedings of the National Academy of Sciences*, 111(10), pp.3663-3670.
- Zhang, Q., Zhou, H., Gao, Q. and Cui, Z. (2014). Analysis of effects of impeller inlet width on the performance of centrifugal pump. *Journal of Chemical and Pharmaceutical Research*, (0975-7384), pp.2078-2081.

